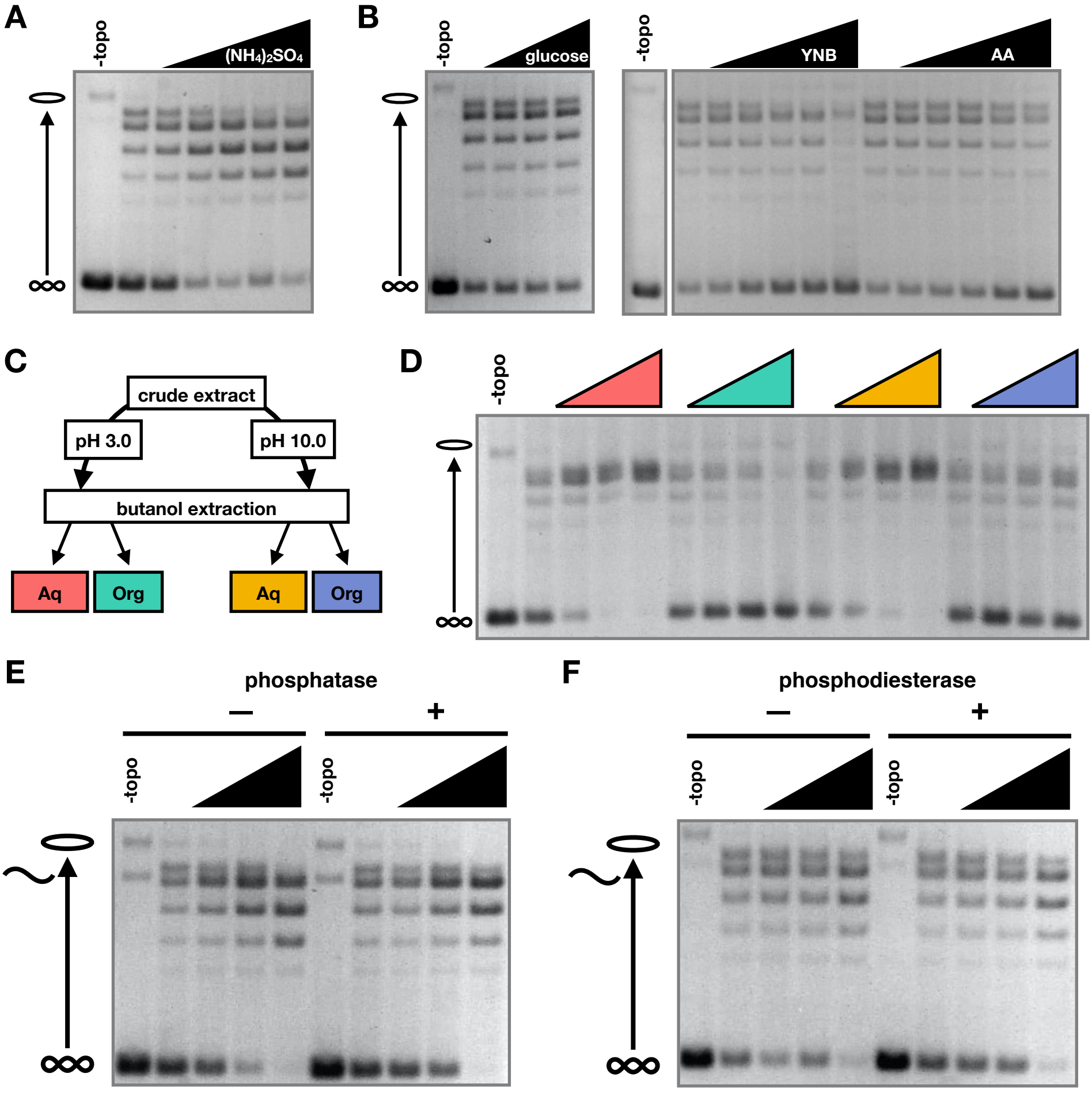

Figure S1. Chemical characterization of stimulatory metabolites, related to Figure 1. Gels show supercoil relaxation activity of *Sc*Top2 at increasing concentrations of additives indicated in each panel. Negative controls with no enzyme (-topo) show the unrelaxed plasmid substrate. (A) $(NH4)_2SO_4$ was titrated from 0 to 50 mM in 10 mM increments. (B) Glucose was titrated from 0 to 40 mg/ml in two-fold increments. Yeast nitrogen base without added sulfate (YNB) and an amino acid mixture containing all 20 amino acids in equal amounts (AA) were titrated from 0 to 10 mg/ml in two-fold increments.(C) Schematic for acid/base butanol liquid-liquid extraction of crude metabolite extracts. 'Aq' indicates the aqueous fraction, and 'Org' indicates the organic fraction. (B) Supercoil relaxation assay with fractions from acid/base butanol extraction as indicated by colors. (C-D) Activity of crude metabolites after enzymatic treatment by Antarctic phosphatase (C) or snake venom phosphodiesterase (D). Lyophilized material from fractions in (D-F) were solubilized in equal volumes of 12.5% DMSO and titrated into relaxation assays in 2-fold dilution steps.

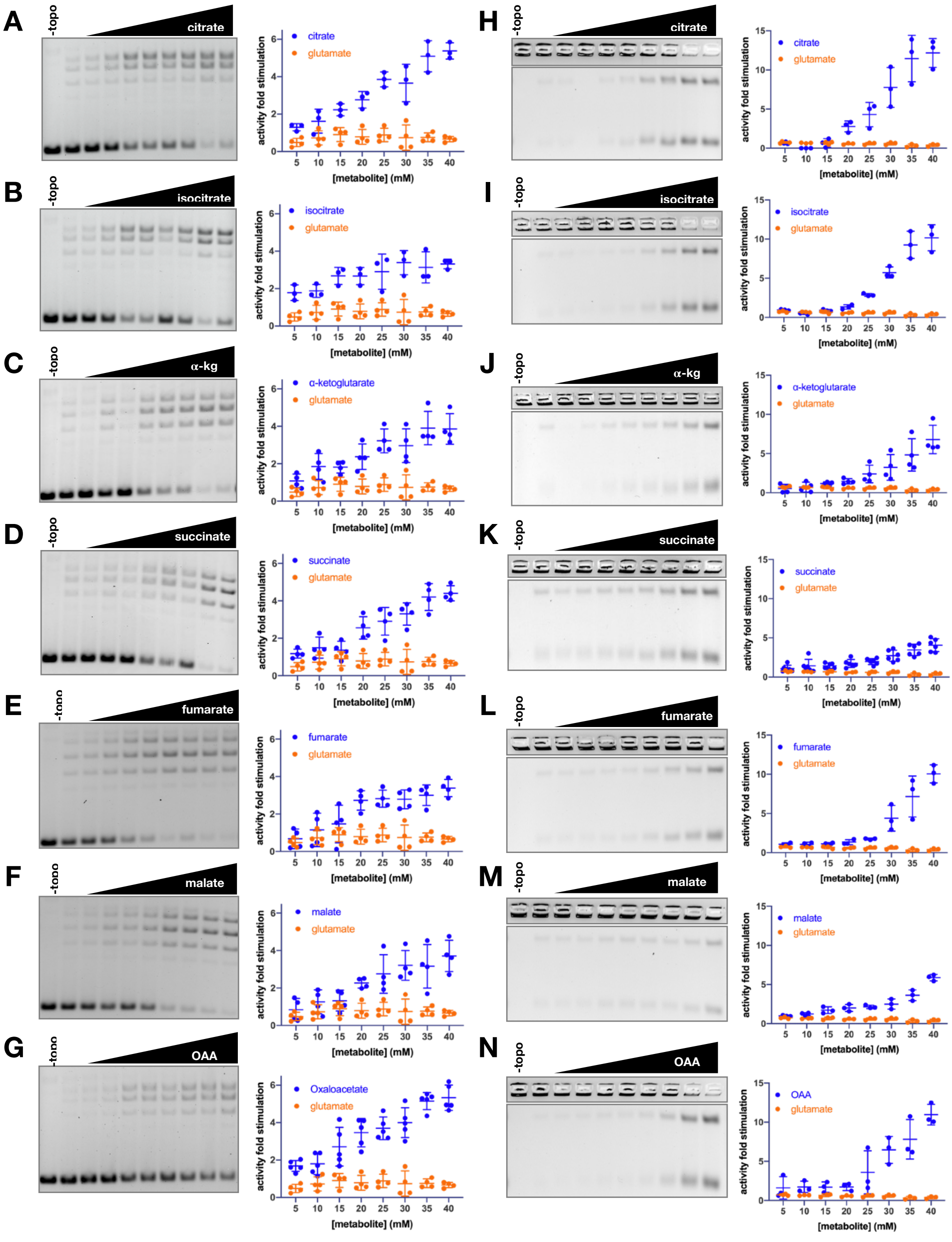

Figure S2. Stimulation of *Sc*Top2 supercoil relaxation activity (A-G) and decatenation activity (H-N) by TCA cycle intermediates (blue) and glutamate (negative control, orange), related to Figure 4. Graphs show mean ± SD of n=3-6 independent experiments.

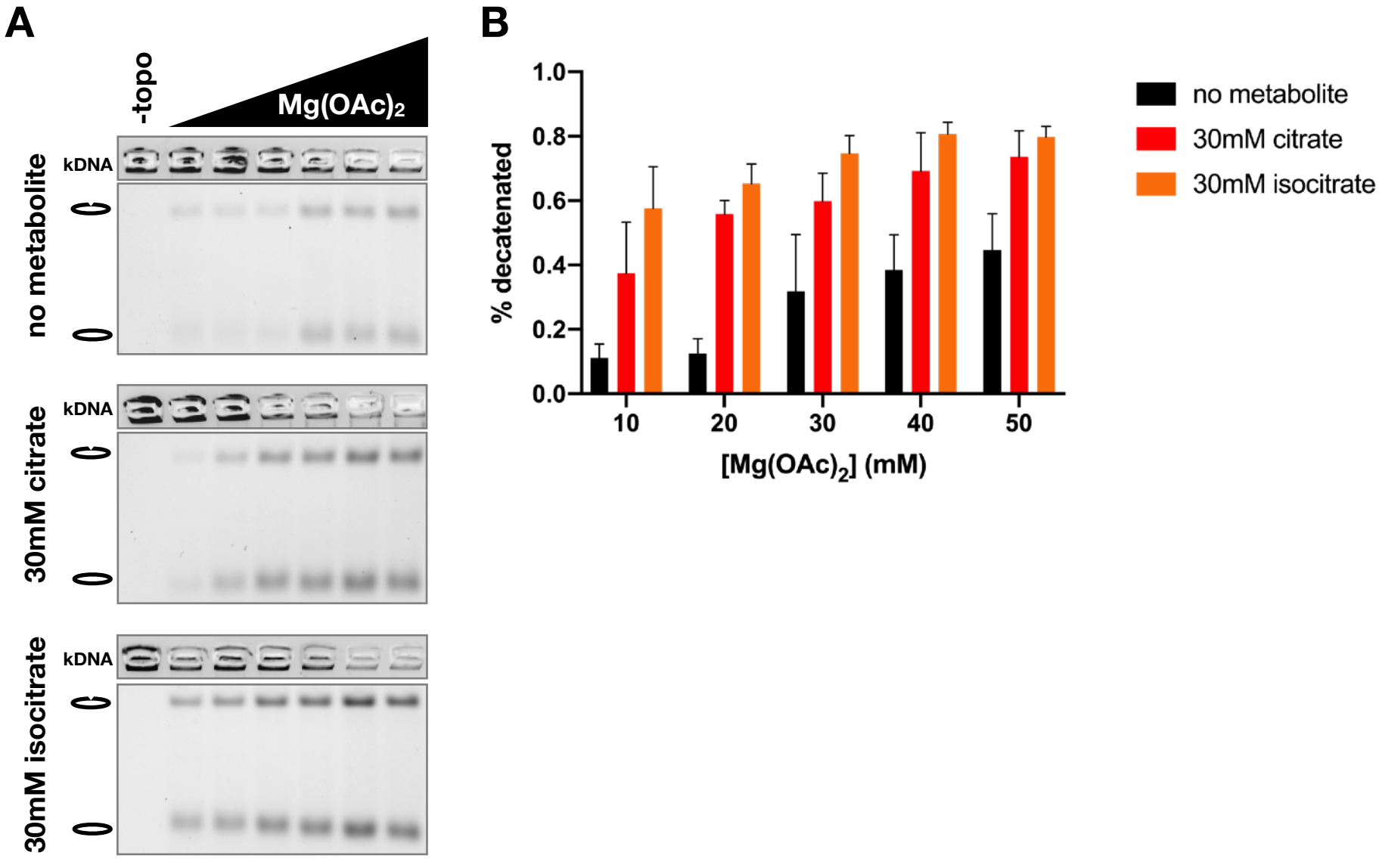

Figure S3. Chelation of Mg^{2+} ions by tricarboxylate TCA cycle intermediates does not affect stimulatory topo II-metabolite interaction, related to Figure 4. (A) Representative gels of decatenation assays performed at different concentrations of $Mg(OAc)_2$ with no added metabolite, 30mM citrate, and 30mM isocitrate. $Mg(OAc)_2$ was titrated from 10 to 50 mM in 10 mM steps. (B) Graphs show mean ± SD of n=3 independent experiments to compare the fraction decatenated under each reaction condition.

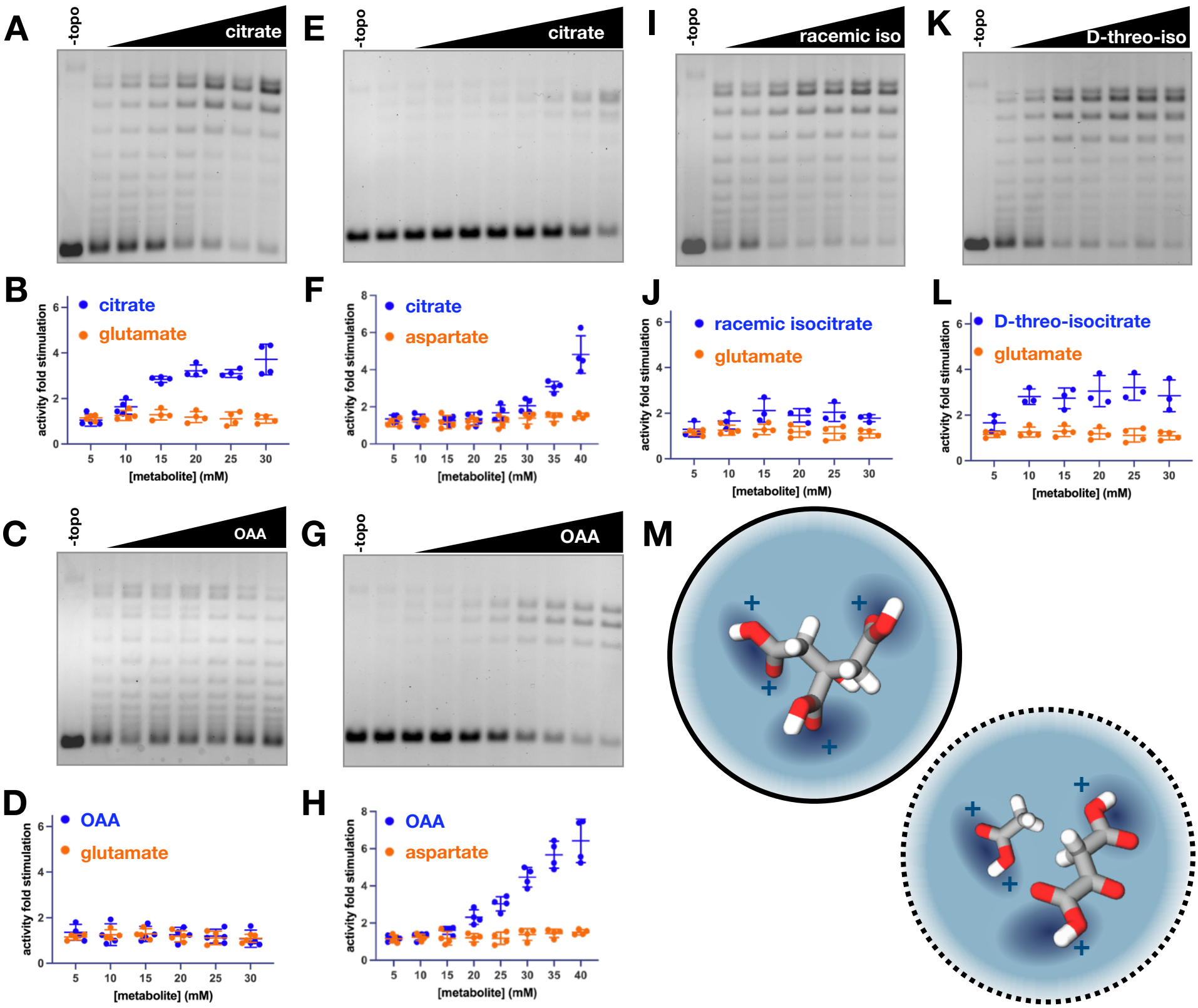

Figure S4. Effect of TCA cycle metabolites on topo II supercoil relaxation activity in different buffer conditions, related to Figure 4. Supercoil relaxation reactions were carried out in 100 mM potassium chloride (A-D & J-M) or 100 mM potassium glutamate (E-H). Glutamate (A-D & J-M) and aspartate (E-H) were included as negative controls. Graphs show mean ± SD of n=3-4 independent experiments. (M) The cartoon inside the solid circle shows citrate in a binding site that engages three carboxylic acid groups. The cartoon inside the dotted circle shows how a small carboxylate buffer molecule such as acetate could allow a dicarboxylic acid such as oxaloacetate (OAA) to engage the tricarboxylic acid binding site to stimulate enzyme activity.

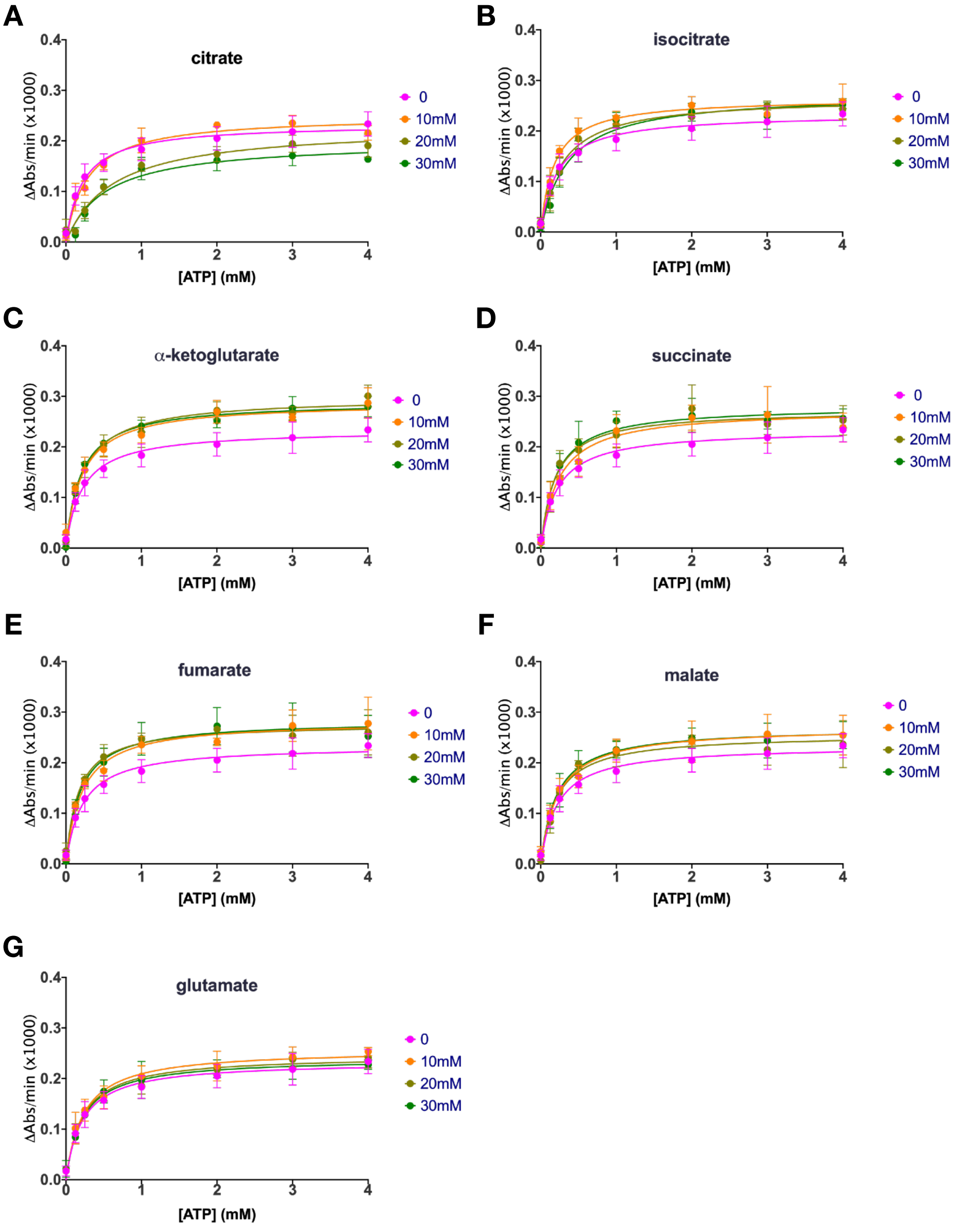

Figure S5. Michaelis-Menten curves of ATP hydrolysis by *Sc*Top2 in the presence of TCA cycle intermediates and glutamate (negative control), related to Figure 4. Rates of ATP hydrolysis were measured in a coupled assay by monitoring NADH consumption as a function of light absorbance at 340 nm wavelength (y-axis). Graphs represent mean ± SD of n=3 independent experiments.

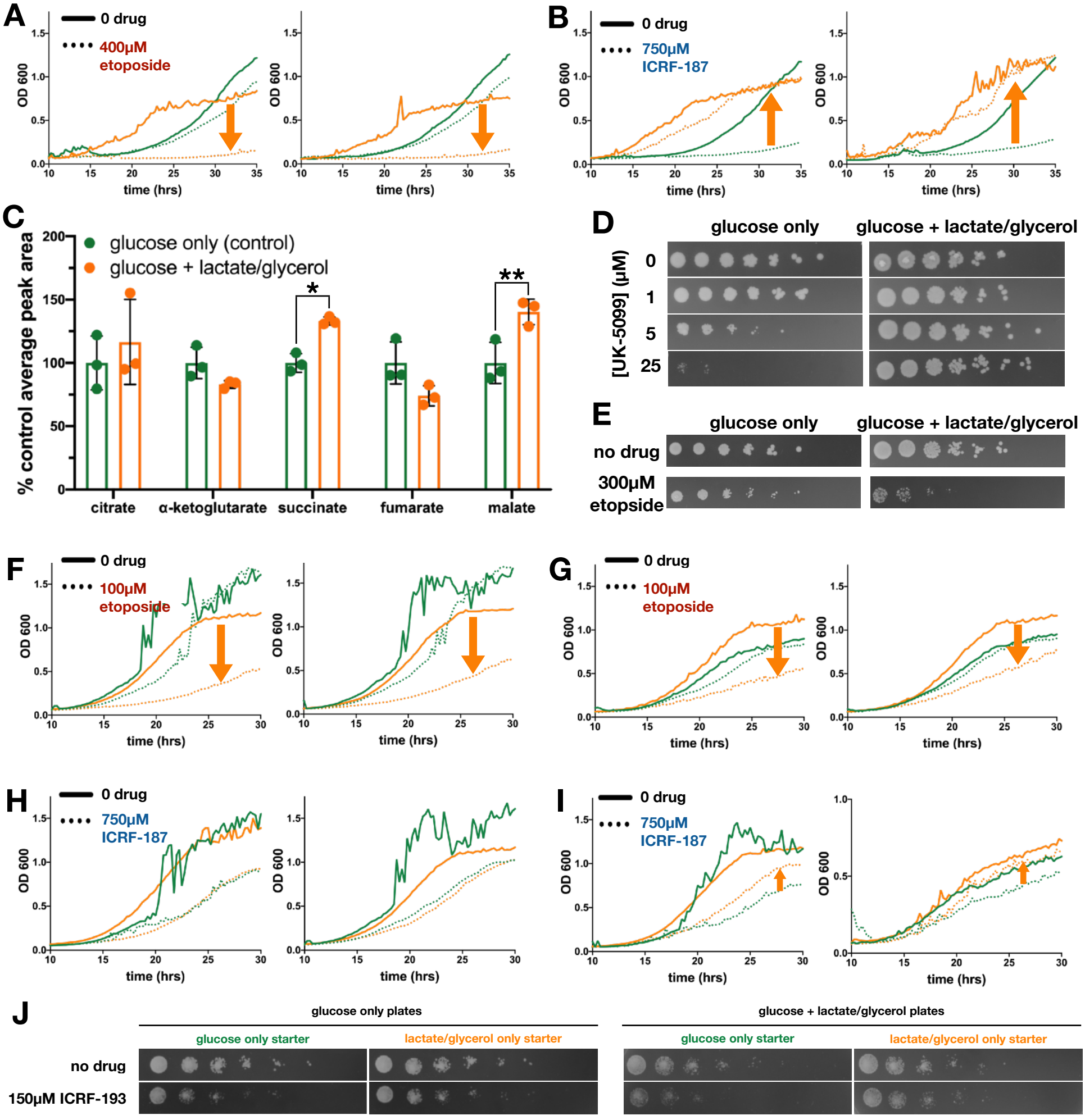

Figure S6. Changes in TCA cycle flux affect sensitivity of yeast to topo II inhibitors - Figure 6 extended data. (A-B) Growth curves of MPC1 (orange) and *mpc1Δ* (green) with etoposide (A) and ICRF-187 (B). (C) Changes in TCA cycle metabolite abundance upon addition of lactate and glycerol to media. Peak areas were normalized to the average of the control condition (glucose only). Bar graphs and error bars indicate mean ± SD of n=3. An unpaired, two-tailed t-test was used to analyze significance of changes peak area. One asterisk (*) indicates $p < 0.05$, and two asterisks (**) indicates $p < 0.01$. (D-E) Serially diluted cultures of yeast were spotted on glucose containing agar plates with and without lactate and glycerol. Spot growth at 0-25 μM UK-5099 (D) and 300 μM etoposide (E) was observed after 2-3 days. (F-H) Growth curves of yeast in glucose-only media (green) or glucose media supplemented with lactate and glycerol (orange). Cultures were inoculated from starters grown in glucose only media (F and H) or lactate and glycerol only media (G and H). Orange arrows show the effect of increasing TCA flux on cytotoxicity of etoposide (F and G) and ICRF-187 (H and I) (downward indicates sensitization and upward indicates rescue). (J) Serially diluted cultures of yeast from either glucose only or lactate/glycerol only starter cultures were spotted on glucose containing agar plates with or without lactate and glycerol. Spot growth on plates with no drug or 150 μM ICRF-193 were observed after 2-3 days.

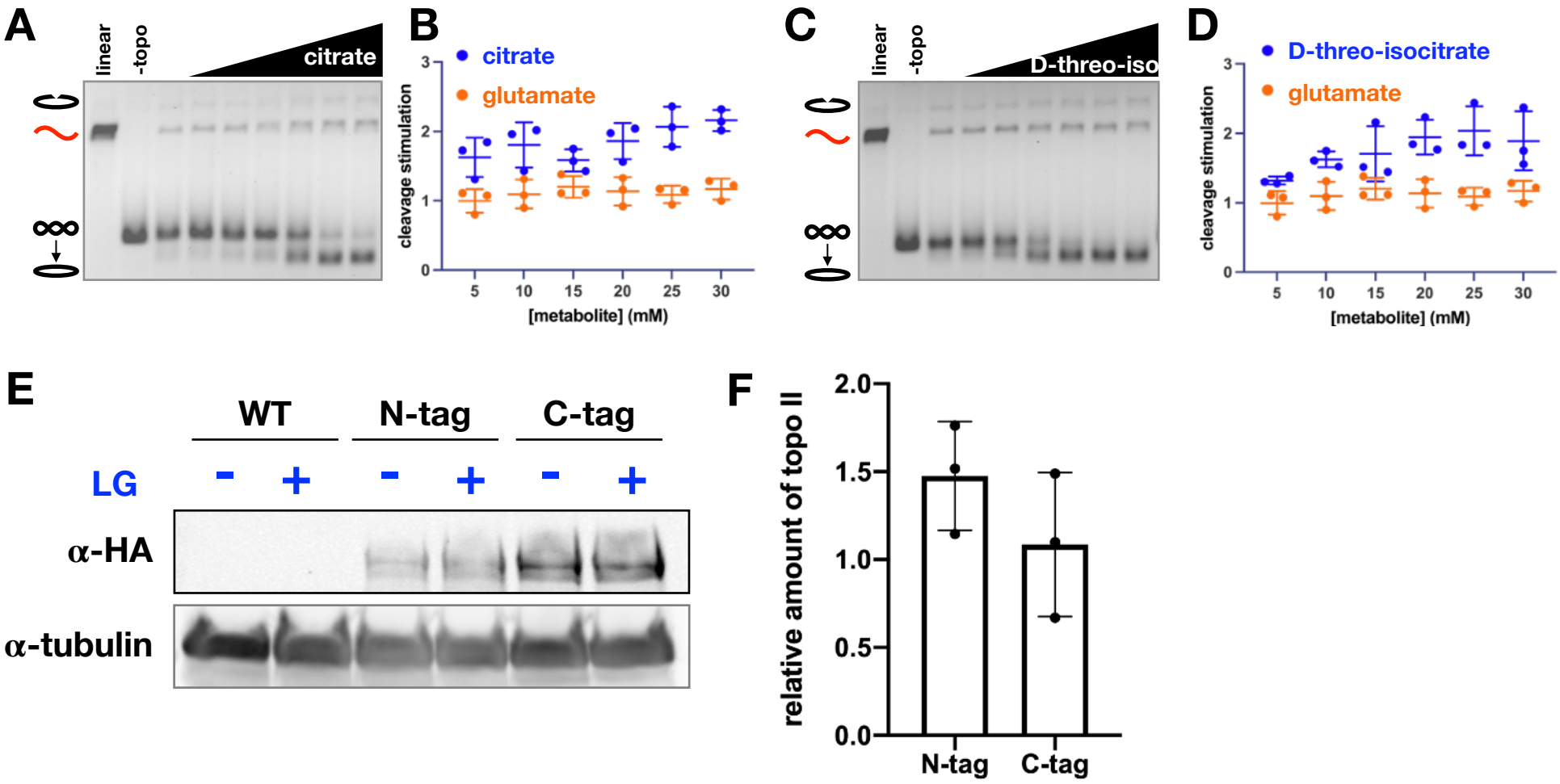

Figure S7. Changes in toxicity of topo II-targeting drugs under different nutrient conditions results from TCA cycle dependent modulation of topo II activity, not topo II expression, related to Figure 7. (A-D) stimulation of topo II activity by TCA cycle intermediates increases formation of etoposide induced double-strand breaks. Citrate (A-B), D-threo-isocitrate (C-D), and glutamate (negative control) were titrated from 0 to 30 mM in 5 mM increments in the presence of 100 μM etoposide. Bands representing nicked, linear, supercoiled plasmid, and relaxed plasmid species are indicated to the left of the representative gels. Graphs show mean ± SD of n=3 independent experiments. (E) Representative western blot of 3xHA-tagged endogenous topo II in an N-terminally tagged (N-tag) or a C-terminally tagged (C-tag) topo II strain from cells grown in media with and without lactate and glycerol (LG). The wildtype (WT) yeast strain (untagged topo II) is shown as a negative control. (F) Quantification of topo II expression levels in the N-tag and C-tag strains. Intensities of the topo II bands were normalized to the corresponding tubulin band. Relative amounts of topo II were calculated by dividing the normalized topo II intensity in the + LG condition to that of the - L/G condition. Data are represented as mean ± SD of n=3 independent experiments

Table S1. Relative abundance of metabolites identified in LC-MS/MS analysis of inactive, stimulatory, and inhibitory fractions of yeast metabolite extracts, related to Figure 3.

LC method	Ion detection mode	Name	Formula	Molecular Weight	RT [min]	Area (Max.)	Log2 Fold Change: (inhibitory/ inactive)	Log2 Fold Change: (stimulatory /inactive)
reverse	negative	[Similar to: L-(-)-Malic acid; ΔMass: -156.0034 Da]	C6 H6 N6 O8	290.02488	2.412	3493395.817	1.26	12.55
reverse	negative	[Similar to: Argininosuccinic acid; ΔMass: -41.9241 Da]	C7 H8 N8 O8	332.04672	2.434	1397237.455	-0.95	11.64
reverse	negative	[Similar to: L-(-)-Malic acid; ΔMass: -171.9772 Da]	C7 H7 N4 O8 P	305.9987	2.402	1112164.887	-0.56	11.03
reverse	negative	[Similar to: Guanidinosuccinic acid; ΔMass: -199.0090 Da]	C8 H20 N6 O5 P2 S	374.06829	2.44	213399.6839	-0.9	9.2
reverse	negative	N-Acetyl-DL-glutamic acid	C7 H11 N O5	189.06284	4.18	307472.4019	1.33	9.18
reverse	negative	[Similar to: L-(-)-Malic acid; ΔMass: -177.9853 Da]	C5 H11 N6 O4 P3	312.00683	2.4	246604.6479	-0.63	9.09
reverse	negative	[Similar to: Ascorbic acid; ΔMass: -7.9652 Da]	C4 H11 O2 P3	183.99733	3.92	434182.1988	-1.42	8.99
reverse	negative	[Similar to: Isocitric acid; ΔMass: -47.9374 Da]	C3 H8 N4 O P4	239.96437	2.352	129109.1578	4.75	8.56
reverse	negative	[Similar to: L-(-)-Malic acid; ΔMass: -171.9681 Da]	C7 H6 N4 O8 S	305.98967	2.408	180057.5437	-0.71	8.44
normal	negative	1-(p-nitrophenyl)-2-amino-1,3-propanediol	C9 H12 N2 O4	212.07895	2.817	458466.9871	-0.15	8.37
normal	negative	L-(-)-Malic acid	C4 H6 O5	134.02014	4.885	22004135.92	-1.87	8.27
normal	negative	2,2'-(Phenylmethylene)bis(4,5-diiodo-3-methyl-1H-pyrrole)	C17 H14 I4 N2	753.73508	6.204	651983.149	-1.21	7.92
reverse	positive	Ureidosuccinic acid	C5 H8 N2 O5	176.04372	2.468	12205186.21	-3.21	7.91
reverse	positive	N-Acetyl-L-glutamic acid	C7 H11 N O5	189.06373	4.296	162775.3558	0.89	7.8
normal	negative	N-Acetyl-DL-glutamic acid	C7 H11 N O5	189.06273	3.564	737450.3103	0.92	6.95
reverse	negative	L-(-)-Malic acid	C4 H6 O5	134.02017	2.423	45982561.9	0.18	6.85

Table S1 (cont).

LC method	Ion detection mode	Name	Formula	Molecular Weight	RT [min]	Area (Max.)	Log2 Fold Change: (inhibitory/ inactive)	Log2 Fold Change: (stimulatory /inactive)
normal	negative	(2R)-2,3-Dihydroxypropanoic acid	C3 H6 O4	106.02514	4.561	1911413.191	-0.86	6.59
reverse	negative	Maleic acid	C4 H4 O4	116.00946	2.419	2577961.827	-0.34	6.4
reverse	negative	2-methylcitric acid	C7 H10 O7	206.04188	4.522	220814.4776	0.21	6.32
reverse	negative	Isocitric acid	C6 H8 O7	192.0261	2.454	382751.7662	-1.84	6.04
reverse	positive	Acetonedicarboxylic Acid	C5 H6 O5	146.02158	3.643	202167.5164	-3.23	4.09
normal	positive	5-Aminolevulinic acid	C5 H9 N O3	131.05771	3.015	5048153.216	2.77	4.08
reverse	negative	Citric acid	C6 H8 O7	192.02613	3.443	4799089.604	-3.87	4.08
reverse	positive	Citric acid	C6 H8 O7	192.02722	3.644	2315923.303	-3.42	3.9
reverse	positive	L-Aspartic acid	C4 H7 N O4	133.0378	2.476	3816610.648	-6.28	3.84
reverse	negative	[Similar to: β-D-Glucopyranuronic acid; ΔMass: -29.9478 Da]	C6 H9 O5 P S	223.99043	2.355	100504.4134	0.41	3.45
normal	positive	5-Aminolevulinic acid	C5 H9 N O3	131.0577	3.342	1273835.534	2.36	3.1
reverse	positive	5-Aminolevulinic acid	C5 H9 N O3	131.05847	2.095	1475777.809	1.01	3.1
reverse	negative	[Similar to: DL-Malic acid; ΔMass: 0.9853 Da]		133.03623	2.431	2092342.63	-7.84	2.92
reverse	positive	L-Alanyl-L-proline	C8 H14 N2 O3	186.10048	2.612	147489.2406	-1.58	2.83
normal	positive	L-Alanyl-L-proline	C8 H14 N2 O3	186.09937	2.99	788432.5397	1.28	2.47
reverse	positive	Y-Aminobutyric acid (GABA)	C4 H9 N O2	103.06382	2.071	2456070.615	0.52	1.87

Table S1 (cont).

LC method	Ion detection mode	Name	Formula	Molecular Weight	RT [min]	Area (Max.)	Log2 Fold Change: (inhibitory/ inactive)	Log2 Fold Change: (stimulatory /inactive)
normal	negative	D-α-Hydroxyglutaric acid	C5 H8 O5	148.0359	4.551	77777.29435	5.14	1.66
normal	positive	Pipecolic acid	C6 H11 N O2	129.07815	7.002	853025411.8	-0.41	1.63